Electron-beam plasma technologies for simulation of environmental effects on satellite surface

N. L. Aleksandrov, M. N. Vasiliev*, S. L. Lysenko*, and S. S. Negodaev**
**Moscow Institute of Physics and Technology*
Dolgoprudny, 141700, Russia

Abstract
The experimental technique was suggested to model the outer space effects on a satellite surface and/or outboard satellite systems. The interaction of the low-pressure electron-beam plasma with a test specimen simulated the effect of fast electron and X-ray irradiation, the effect of surface electrical charging and the action of the chemically active oxygen in spaceflight. One specimen side was uniformly or locally heated by the electron beam bombardment and the opposite one could be cooled by a special cryostat. The preliminary results of the measurement of the temperature distribution over stainless steel and aluminium discs subjected to a quasi-stationary 30 keV electron beam in the chamber filled with rarefied oxygen were presented. The computer simulation of the electron beam propagation in the gas and of the oxygen plasma generation was carried out to calculate the spatial temperature distributions both over the disc and in the plasma near the disc surface. The calculated temperature distributions were compared with the measured ones. The fluxes of some active heavy plasma particles bombarding the specimen surface were calculated as well.

1. Introduction

Different factors of a spaceflight can affect the operation and characteristics of spacecraft control systems. Various test techniques have been suggested to model the space radiation effects and some other harmful environment effects on satellites in a ground-based laboratory. These effects are the impact of the fluxes of high-energy particles and electromagnetic radiation in a wide range of wavelength (from X- up to IR-rays), intensive heating and “space cold”, chemical interaction between the spacecraft surface and the surrounding atmosphere, etc. Thus, the problem is to accomplish the combination of numerous spaceflight effects using a single laboratory setup.

The electron-beam technologies seem to be promising to simulate the combined action of the environment on the satellite surface or on the outboard systems (sensors, antennas, etc). The possibilities of this approach, the pilot experimental setup, and the data of the preliminary experiments in comparison with the results of the computer simulations are described in the present paper.

2. Simulation of spaceflight factors with electron-beam technology

Our approach is based on the unique properties of the electron-beam plasma (EBP) and advantages of the EBP generation (see, e.g., [1]). A typical electron-beam set-up contains the high-energy electron beam generator equipped with an injection window through which the beam is injected into the chamber filled with a gas or gas mixture. Practically any gas is applicable for the EBP generation; the pressure in the working chamber can be varied from 10^{-5} to 10^{3} Torr. A test specimen is placed into the chamber. Location of the specimen and the ways to fix it can be different depending on the purpose of the study.

The electron-beam technique is able to simulate the following spaceflight factors affecting the test specimen surface.

(a) Thermal action. Both uniform and specially distributed local heating of the surface can be obtained by means of the electron beam. In particular, time-varying or cyclic thermal tests could be carried out, as well as the tests in which one side of the specimen is subjected to a high thermal flux, whereas the other side is “space cold”, the conditions typical for spaceflights.

(b) High-energy electron radiation. Modern accelerators are able to generate electrons over all practically important energy range, from tens of kilovolts to a few megavolts.

(c) X-ray radiation. Under the conditions considered, X-rays could be emitted when decelerating high-energy electrons in special targets. The radiation spectrum and intensity are controlled by varying electron energy, electron beam current and the target material.

(d) Interaction between the spacecraft surface and its own atmosphere. This atmosphere is imitated by filling the working chamber with special gas mixture and/or by vaporization and ablation of specimen material due to the high-energy electron irradiation. It should be noted that it is possible to study the interaction between the test specimen and plasma generated in its own atmosphere.

(e) The effect of atomic oxygen and of its plasma. Atomic oxygen is a dominant gas species in the Earth's atmosphere at altitudes in the range 300-800 km. These altitudes are typical for the orbits of a large number of spacecraft used for various purposes.

(f) The effect of surface electrostatic charge. In sufficiently high-altitude orbits, the surface potential of a spacecraft can reach tens of kilovolts. Due to the differential charging of the dielectric surfaces of the spacecraft, the potential difference between its various elements can reach the electrical breakdown threshold. This leads to surface discharges generating electromagnetic, optical and acoustic interferences for spacecraft equipment. The electrostatic charging of the spacecraft affects the interaction between the surface and plasma particles and consequently influences plasmachemical processes near the surface. And vice versa, the modification of the electrophysical properties of the materials subjected to plasma action for a long period of time could influence the ability of the material to resist interferences and electrical breakdown. The electron beam technique was proved to be promising to simulate the spacecraft differential charging.

(g) Plasma-stimulated luminescence. The luminescence of elements of a spacecraft could affect the operation of the outboard optical devices and sensors. A change in colour of the surface layers of optical materials caused by their chemical or plasmachemical interaction with the ambient atmosphere could interfere with the operation of these systems as well.

3. Experiment

Figure 1 shows the scheme of the experimental setup, which is used to study the above-listed effects in various combinations. Here, the test specimen (1) is mounted on the thermal table, which contains two cooling devices, the circulation cryolite (6) and the additional refrigerator (4) using Peltye's elements. The left side of the test specimen is heated by the scanning electron beam (3), which is generated by the electron-beam gun (1). The gun has a control system to govern the beam current and to scan and focus the beam in different manners. The energy of beam electrons is varied by changing the accelerating voltage supplied to the gun by the high-voltage power source.

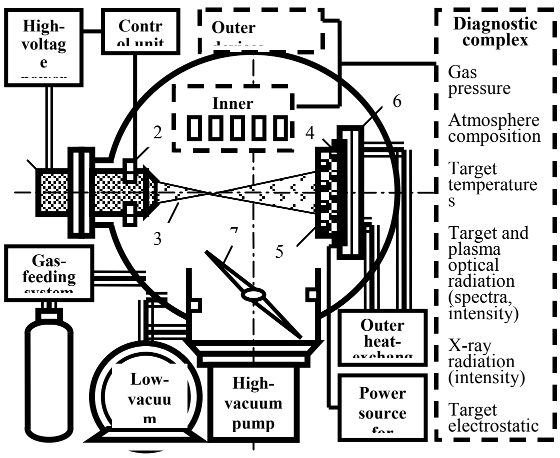

Figure 1: Scheme of the experimental setup to study the electron beam interaction with the test specimen and ambient gas in various heating/cooling regimes.

The gun and thermal table are placed into a low-pressure working chamber continuously evacuated by the turbo-molecular pump. The chamber is filled with the gas or gas mixture, the pressure and gas mixture composition being maintained automatically. The electron beam ionizes the gas and, as a result, a weakly-ionized non-equilibrium plasma is generated. The active charged and neutral particles produced in the plasma fall on the specimen surface and possibly react with it.

Sensors are placed inside the chamber to measure the gas and specimen parameters and to process primary information. Some devices are mounted outside the chamber and are connected with the interior sensors via fibre-optical lines and power cables. For this purpose, the camera has sealed connectors. Figure 1 shows a list of parameters to be measured and figure 2 shows the scheme of the measurement of the specimen temperature.

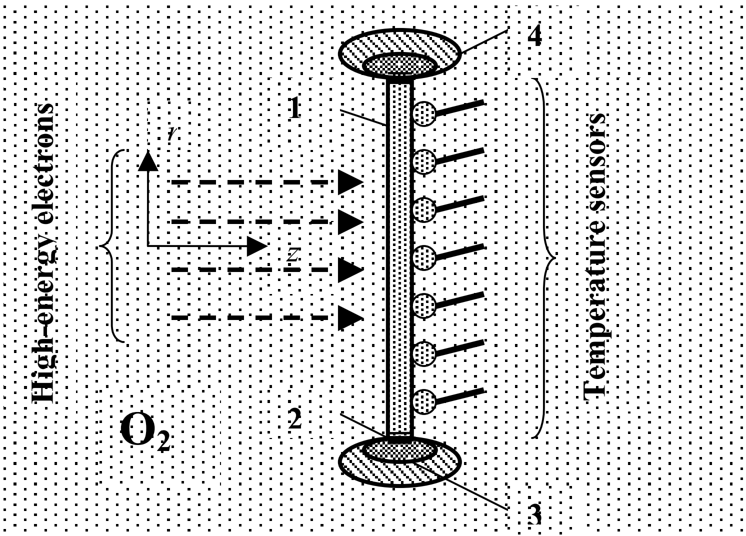

Figure 2: Scheme of the specimen temperature measurement: (1) test specimen, (2) heat conductive paste, (3) flowing water, and (4) circular heat-exchanger.

The following parameters could be realised in the experiment.
- Electron beam energy (E_b) in the range 25-60 keV.
- Electron beam current (I_b) in the range 1-100 mA.
- Gas pressure (P) in the range 10^{-6} - 5×10^{-4} Torr. The values of P can be increased up to 50 Torr if the electron beam is injected into the chamber through the gas-dynamic injection window [1].
- Temperature of the cooled surface can be decreased down to –55 C.
- Temperature (T) of the heated surface can be increased up to 120 C. The local temperature of a gas subjected to an electron beam can be increased up to 500 C.

4. Computational model

A computer model has been developed to simulate interactions between the electron beam, the plasma in the chamber and the specimen. This model was similar to that used in [2, 3] and considered the scattering of high-energy electrons in the gas and solid body, the gas heating due to dissipation of the electron beam energy, the rebound and absorption of high-energy electrons on the specimen surface, and the specimen heating by the plasma and/or beam electrons. The heat transfer in the gas and the solid body and between the plasma and the solid body due to thermal conductivity and radiation is responsible for the specimen heating/cooling. Also the model considers the diffusion of charged and neutral particles and the production and loss of active neutral and charged species in the gas subjected to the electron beam.

To describe the interaction of an electron beam with the gas and solids the following physical model was used. A thin cylindrical electron beam was assumed to be injected into the working chamber, filled with the gas, along its axis. When propagating throughout the gas, the electrons underwent elastic, inelastic, and ionizing collisions with the gas molecules; the latter gave rise to the secondary electrons. In the absence of an external electric field, the electrons between the collisions moved along straight lines. Due to the collisions, the electron changed the propagation direction and partially lost its energy. The energy loss depended on the kind of the process. As a result, the electrons propogated along a polygonal line as long as they reach the chamber wall or the specimen surface. Then, the electron motion in solid body should be described in the same way but the parameters characterizing the medium must be changed. The simulation of the electron trajectory stopped when the electron energy became lower than 150 eV.

When simulating the electron motion in the gas, variations in the gas density due to its nonuniform heating by the beam should be taken into account. To do this, the gas density at a particular point was determined for a particular gas pressure and calculated temperature in terms of the equation of state. Self-consistency in the simulating procedure was achieved as follows. First, the electron propagation in the gas and in the solid material was calculated using the Monte Carlo method. The acquired data were then statistically processed and the spatial distribution of the heat released in the gas and at the wall surface was simulated. Finally, the temperature distribution and the gas density were determined throughout the entire volume including the specimen bulk. The above procedure was repeated after calculating each ten trajectories; the simulation of 100 trajectories gave a quasi-steady state temperature distribution. The temperature relaxation also ocurred due to the conductive and radiative heat transfer between different parts of the inner surface of the working chamber. These mechanisms partially balanced the nonuniformity of the energy deposition caused by insufficient statistics. In practice, from 5000 to 500 000 trajectories were simulated to obtain smooth spatial distributions of the ionization rate whereas a quasi-steady state temperature distribution in the working chamber was established after the calculation of only 100 trajectories.

The simulations showed that the electron beam can burn the “channel” in the gas bulk. In the channel the gas density was significantly lower than that in entire gas volume because the electron beam effectively heated the gas near the axis of the EBP cloud where the electron-beam current density was the highest. This led to an increase in the penetration depth of the high-energy electrons in the direction of the electron beam propagation.

Using the collected statistical data the distributions of the ionization and excitation rates of the neutral particles over the chamber volume were found; the electron beam power absorbed by a unit gas volume and unit area of the the chamber or the specimen surface were found as well. These data were then used to calculate the densities of atoms, excited molecules and charged particles produced by the electron beam. The calculations were carried out for a pure molecular oxygen under the conditions corresponding to the experimental ones. The kinetic scheme included 12 components and 39 reactions. The components under consideration were O_2, O, O_3, $O_2(a^1\Delta_g)$, e, O^+, O_2^+, O_4^+, O^-, O_2^-, O_3^-, and O_4^-. The rate coefficients were taken from [4], whereas the rates of O_2 excitation, dissociation and ionization by high-energy electron impact were calculated according to [5]. The balance equations for the neutral and charged species were numerically solved assuming the diffusion of charged plasma particles to be ambipolar.

5. Calculated and experimental results

To demonstrate the applicability of the EBP technologies for the satellite system tests and to verify the developed computer simulation method the heating of a flat specimen placed in the oxygen plasma was studied. The fluxes of active charged and neutral particles falling on the specimen surface were calculated as well. Figure 3 shows the radial temperature distributions over a 2 mm thick metallic disc 150 mm in diameter for different gas pressures.

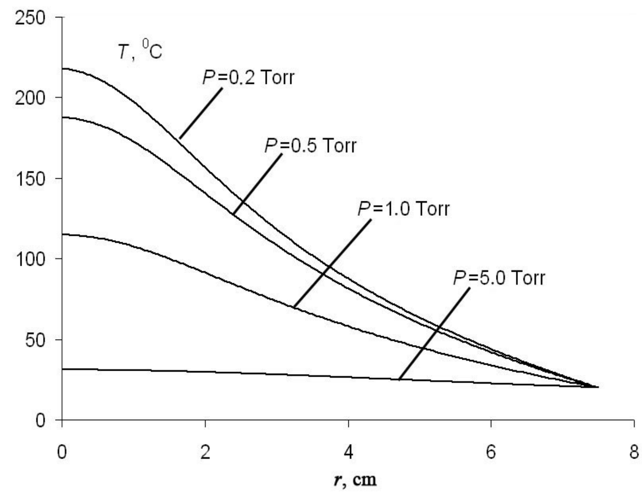

Figure 3 : The calculated radial distributions of the temperature over a 2 mm thick disc 150 mm in diameter made of an aluminium alloy. The disc is placed in the oxygen EBP at the distance from the injection point z_d = 25 cm.

The disc was made of an aluminium alloy D16 and was placed into the chamber filled with molecular oxygen, which was ionised by the electron beam. The axis of the beam injection and the disc axis coincided, the distance between the injection window and the disc plane being z_d = 25 cm. The electron beam energy was E_b = 30 keV and the beam current was I_b = 10 mA. The temperature of the cylindrical side surface of the disc was assumed to be 20°C. The figure shows the characteristic disc temperature to increase as the gas pressure drops because at lower pressures a smaller percentage of the electron beam power is absorbed by the gas-dynamic injection window and by the gas and, therefore, the disc absorbs a larger percentage of the beam power.

Figure 4 presents the comparison between the calculated and measured radial distributions of temperature over the thin disc of the same dimensions made of steel X18H10T. The electron beam parameters were the same as above, whereas the distance between the injection point and the disc plane was decreased to z_d = 15 cm. The figure shows the calculated and measured temperature distributions to be in good agreement. As the gas pressure increased the temperature distributions over the disc became more uniform.

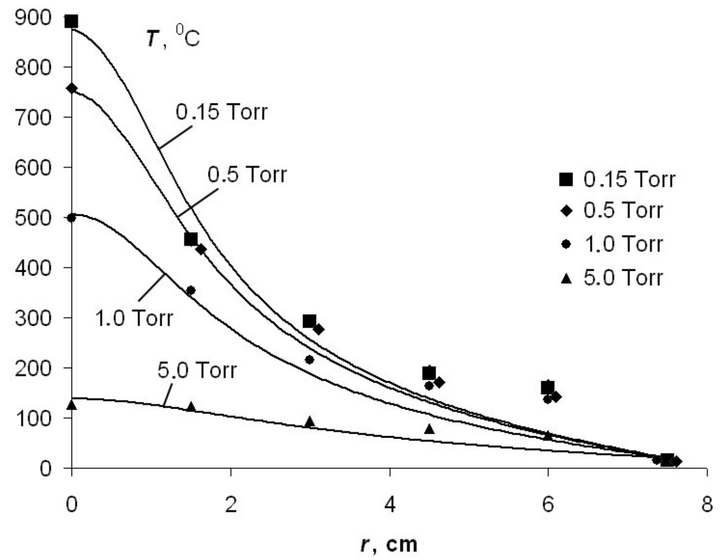

Figure 4 : The radial distributions of the temperature over a 2 mm thick stainless-steel disc 150 mm in diameter placed in the oxygen EBP at the distance from the injection point z_d = 15 cm. The curves represnt the calculation results and the markers represent the experimental data.

The calculated radial distributions of the fluxes of selected active species (electrons, positive ions, O atoms and $O_2(a^1\Delta_g)$ molecules) falling on the disc surface are given in Figure 5. The fluxes were calculated using the values of thermal velocity for a particle of each kind. It was assumed that the total fluxes of negatively and positevely charged particles are approximately equal ; this is due to the charging of the surface by mobile electrons. The fluxes of the neutral particles were more intensive than those of the charged particles. The dominant active species were O atoms. The flux of $O_2(a^1\Delta_g)$ molecules was less intensive than that of O atoms by a factor of three, whereas the fluxes of charged particles were an order of magnitude weaker.

The densities and fluxes of O atoms produced under the conditions considered can be five orders of magnitude higher than those under real conditions of a spaceflight. Therefore, the annual dose of O-atom irradiation accumulated by the satellite in the flight could be obtained under the laboratory conditions for significantly shorter time period (about ten minutes).

The fluxes of active species on the disc surface depend on the properties of the electron-beam-sustained plasma produced in the working chamber. The density of deposited power along the electron-beam axis was approximated as $Q = A(P, z)/z^2$, where P is the gas pressure and the coefficient $A(P, z)$ depends on the distance from the injection point, z, only slightly. Figure 6 shows this dependence at various gas pressures. The value of A was almost independent of z at 1 Torr. An increase in the gas pressure to 5 Torr led to much more pronounced attenuation and scattering of the electron beam. As a result, the value of A decreased with increasing z. Near the disc surface, the value of A could increase with z due to the rebound of the high-energy electrons from the surface.

Figure 7 shows the longitudinal distribution of the gas temperature, T, along the axis of the electron beam at 1 and 5 Torr. The attenuation and scattering of high-energy electrons in the gas were inefficient at 1 Torr. In this case, the value of T was almost independent of z and increased only near the disc surface due to the heat transfer from the disc intensively heated by the electron beam. This effect was not observed at 5 Torr because at this pressure the electron beam was strongly attenuated and scattered in the gas and the disc heating was negligible (see figure 3). At higher pressures the gas absorbs the main portion of the electron beam power at the first centimetres of the beam range and the value of T decreases at longer z.

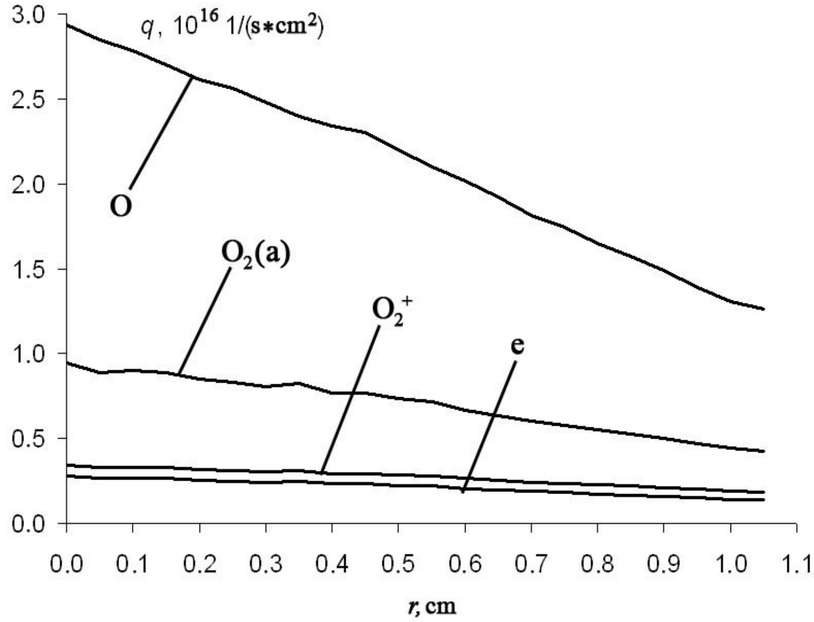

Figure 5 : The calculated radial distributions of the active species fluxes falling on the surface of a 2 mm thick stainless-steel disc 150 mm in diameter placed in the oxygen EBP at P = 5 Torr ; E_b = 30 keV and I_b = 10 mA. The distance between the injection window and the disc plane is z_d = 15 cm.

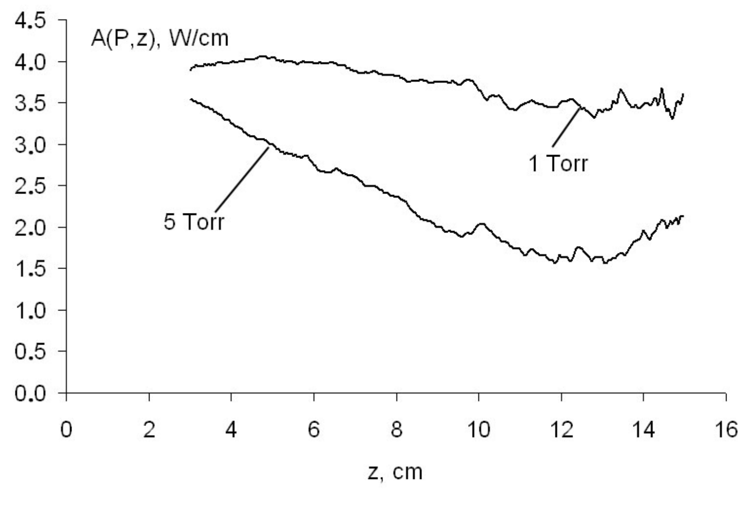

Figure 6: The coefficient $A(P, z)$ as a function of the distance from the electron-beam injection point at E_b = 30 keV, I_b = 10 mA, and P = 1 and 5 Torr. The distance between the injection window and the disc plane is z_d = 15 cm.

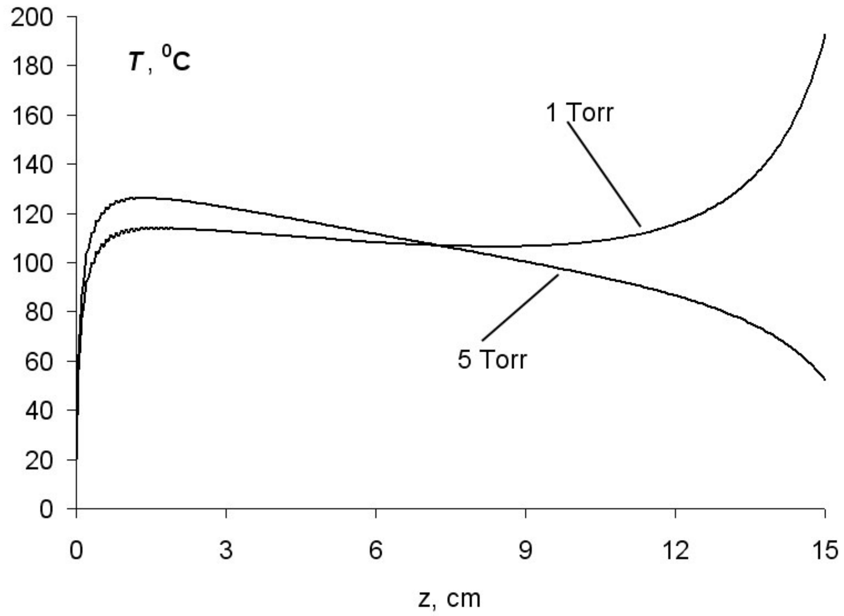

Figure 7 : The gas temperature in the electron-beam-sustained plasma at E_b = 30 keV, I_b = 10 mA and various gas pressures as a function of the distance from the electron-beam injection point. The distance between the injection window and the disc plane is z_d = 15 cm.

Figure 8 shows the radial distributions of the electron density in the electron-beam-sustained plasma for various distances from the injection point at 5 Torr. Under the conditions studied, the peak electron density was reached at a distance of several centimetres from the injection point. The radius of the plasma cloud was around 0.5 cm.

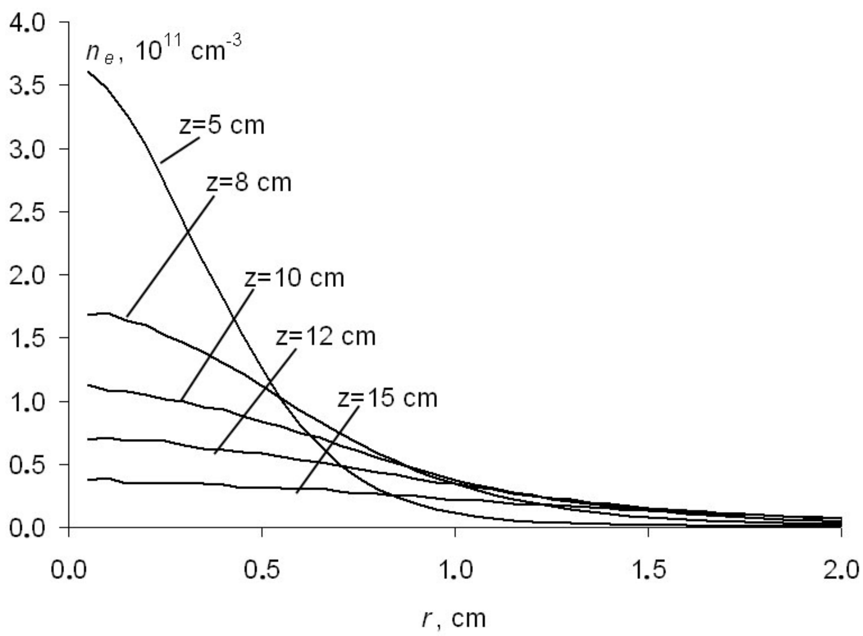

Figure 8: The radial distributions of the electron density in the electron-beam-sustained plasma at E_b = 30 keV, I_b = 10 mA, P = 5 Torr and various distances from the electron-beam injection point. The distance between the injection window and the disc plane is z_d = 15 cm.

Table 1 shows the composition of the plasma generated in the gas by the electron beam near the centre of the disc. Here, the predominant charged components were electrons and O_2^+ ioms at 1 Torr, whereas at pressures about 5 Torr the electron density and the density of negative ions were of the same order of magnitude. The increase in the density of negative ions at higher pressures is associated with three-body electron attachment to O_2 molecules and with the formation of negative ions O_2^- in the reaction $2O_2 + e \rightarrow O_2^- + O_2$.

Table 1: Densities of charged species in the electron-beam-sustained oxygen plasma near the centre of the disc specimen at various gas pressures.

Species	e	O_2^+	O^+	O_4^+	O^-	O_2^-	O_3^-	O_4^-
1 Torr	1.51×10^{11}	1.49×10^{11}	1.90×10^{9}	1.22×10^{7}	3.76×10^{7}	2.96×10^{7}	2.17×10^{4}	4.98×10^{2}
5 Torr	3.75×10^{10}	5.81×10^{10}	1.64×10^{8}	6.63×10^{9}	1.63×10^{9}	7.90×10^{9}	1.78×10^{10}	6.52×10^{7}

6. Conclusions

The experimental technique to model the outer space effects on the satellite surface and/or the outboard satellite systems at the height 300-800 km was suggested. The interaction of the low-pressure electron-beam plasma with the test specimen simulated the fast electron and X-ray irradiation, the surface electrical charging and the action of chemically active oxygen. The preliminary experiments in which the combined action of the specimen heating and surface plasmachemical processes with O atoms had been carried out successfully.

The kinetic model was developed to simulate numerically the properties of the electron-beam plasma in pure molecular oxygen and the interaction between the plasma and the surface of a solid body. The properties of the plasma generated in the gas under the action of the electron beam and the heating of the metal disc by the high-energy electron beam were studied at various gas pressures. The calculated radial temperature distributions over a disc specimen were in good agreement with the measurements.

References

[1] Vasiliev, M. N., and A. H. Mahir. 2008. Electron–beam plasma systems in industrial and aerospace applications. *Publ. Astron. Observatory Belgrade.* 84:421-425.
[2] Vasilieva, T. M., S. L. Lysenko, and V. A. Kukarenko. 2010. Plasma assisted synthesis of oxides on inner surface of titanium tubes. *Fizika i khimiya obrabotki materialov*. 5:29-36.
[3] Aleksandrov, N. L., M. N. Vasiliev, S. L. Lysenko, and A. Kh. Makhir. 2005. Experimental and theoretical study of a quasi-steady electron-beam plasma in hot argon. *Plasma Phys. Rep.* 31:425-435.
[4] Kossyi, I. A., A. Yu. Kostinsky, A.A. Matveyev, and V. P. Silakov. 1992. Kinetic scheme of the non-equilibrium discharge in nitrogen-oxygen mixtures. *Plasma Sources Sci. Technol.* 1:207-220.
[5] Konovalov, V. P., and E. E. Son. 1987. Electron degradation spectra in gases. In.: *Chemistry of plasma*. Ed. B. M. Smirnov. Moscow: Energoatomizdat. 14:194-227.